Disclaimer

This note has not been internally reviewed by the DØ Collaboration. Results or plots contained in this note were only intended for internal documentation by the authors of the note and they are not approved as scientific results by either the authors or the DØ Collaboration. All approved scientific results of the DØ Collaboration have been published as internally reviewed Conference Notes or in peer reviewed journals.

DØ Note 2786

Fermi National Accelerator Laboratory

FERMILAB-Conf-95/276-E

CDF and DØ

Observation of the Top Quark

S.B. Kim
Presented for the CDF and DØ Collaborations

Fermi National Accelerator Laboratory
P.O. Box 500, Batavia, Illinois 60510

Randall Laboratory
University of Michigan
500 E. University Street
Ann Arbor, Michigan 48109

August 1995

Published proceedings from the *15th International Conference on Physics in Collision*, Cracow, Poland, June 8-10, 1995.

Disclaimer

CDF/PUB/TOP/PUBLIC/3302
DØ/PUB/TOP/PUBLIC/2693
FERMILAB-CONF-95/276-E

Observation of the Top Quark

Soo-Bong Kim (CDF)
Randall Laboratory, University of Michigan
500 E. University St., Ann Arbor, MI 48109, USA
Presented for the CDF and DØ Collaborations

Published Proceedings 15th International Conference on Physics in Collision, Cracow, Poland, June 8-10, 1995

Abstract

Top quark production is observed in $\bar{p}p$ collisions at $\sqrt{s} = 1.8$ TeV at the Fermilab Tevatron. The Collider Detector at Fermilab (CDF) and DØ observe signals consistent with $t\bar{t}$ to $WWb\bar{b}$, but inconsistent with the background prediction by 4.8σ (CDF), 4.6σ (DØ). Additional evidence for the top quark is provided by a peak in the reconstructed mass distribution. The kinematic properties of the excess events are consistent with the top quark decay. They measure the top quark mass to be 176 ± 8(stat.)±10(sys.) GeV/c^2 (CDF), 199^{+19}_{-21}(stat.)±22(sys.) GeV/c^2 (DØ), and the $t\bar{t}$ production cross section to be $6.8^{+3.6}_{-2.4}$ pb (CDF), 6.4 ± 2.2 pb (DØ).

1 Introduction

The top quark is required in the standard model (SM) as the weak-isospin partner of the bottom quark. The existence of the top quark was indirectly proved by the absence of flavor-changing neutral currents in b-flavored meson decays[1] and the forward-backward asymmetry measured in $e^+e^- \rightarrow b\bar{b}$[2].

Recently the CDF collaboration presented the first direct evidence of the top quark production with a statistical significance of 2.8 standard deviations, a top quark mass $174 \pm 10^{+13}_{-12}$ GeV/c^2, and a production cross section of $13^{+6.1}_{-4.8}$ pb[4]. The DØ collaboration published a lower limit on the top quark mass of 131 GeV/c^2, at a confidence level (CL) of 95%[5]. A subsequent publication[6] reported the top quark production cross section as a function of the assumed top quark mass.

Top quarks are expected to be produced predominantly by a pair production process, shown in Fig. 1, from $\bar{p}p$ collisions at the Tevatron energy 1.8 TeV. A top pair decays, according to the minimal SM, into a W pair and two b quarks; $t\bar{t} \rightarrow W^+bW^-\bar{b}$. The W bosons subsequently decay into either two quarks (W hadronic decay) or a lepton plus a neutrino (W leptonic decay). Two-thirds of W bosons decay hadronically, and the quarks are seen as jets - large numbers of particles directed in fairly narrow but ill-defined cones along the initial directions of the quarks. Gluons radiated by QCD processes in $\bar{p}p$ collisions are also seen as jets, and therefore it is difficult to separate two jets of a W decay from QCD gluon jets. On the other hand, leptonic decays of W into a high-energy lepton and an associated neutrino tend to have characteristics of being well separated from hadronic backgrounds: a large, well isolated energy deposited by the lepton and missing energy ($\not\!\!E_T$) into the transverse direction of the beam due to the undetected neutrino.

Both CDF and DØ require a W decay candidate from the t or $\bar{t}$. Events where both W bosons decay leptonically into $e\nu$ or $\mu\nu$ are called "dilepton" events ($e\mu, ee, \mu\mu$). Those where one W decays leptonically and the other decays into quarks - which appear as jets in the detector - are called "lepton plus jets" events (e, μ+jets). The "dilepton" channel is very clean due to a requirement of two leptons, but has a small branching ratio (5%) of $t\bar{t}$ decays. The "lepton plus jet" channel has a rather higher branching ratio (30%), but suffers from a large W+multijet background.

Background in the lepton+jets mode can be further reduced if one identifies the b quark from the top decay. The b-quark identification can be done either by finding a b-decay vertex displaced ($\sim$ 4 mm) from a primary $p\bar{p}$ collision vertex due to its lifetime ($\sim$ 1 ps) or by looking for the lepton from a b "semileptonic" decay into a lepton, a neutrino and hadrons. CDF can

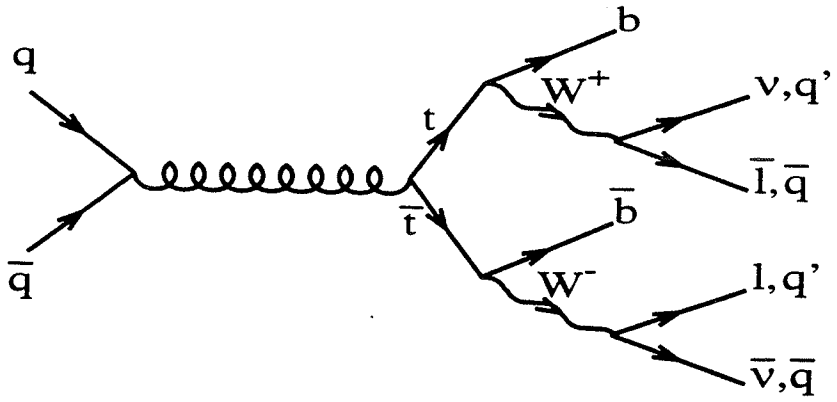

Figure 1: Top quark production by $q\bar{q}$ annihilation, followed by the standard model decay of the $t\bar{t}$ pair.

measure the displacement of the b-decay vertex from the main interaction vertex (SVX tag). DØ can not currently find b-decay vertices, although the group plans to install a silicon vertex detector before the next Tevatron collider run. Both CDF and DØ also look for the semileptonic decays of b quarks from the t or $\bar{t}$. Those decays are identified by a "soft" lepton (e or μ at CDF, only μ at DØ) with an energy less than is typical of weak boson decay.

Without a silicon vertex detector, DØ obtains a strong discrimination between background and signal events by requiring that an event must have a minimum transverse energy - so called "H_T" (transverse hadronic energy). Because CDF can efficiently detect the b quark from the top decay, the group can isolate a top signal without demanding such a transverse-energy requirement although they examine the transverse-energy distribution of their signal.

Here I describe CDF and DØ observations of the top quark production (see References [7] and [8]) based on data collected at the Fermilab Tevatron at $\sqrt{s} = 1.8$ TeV with integrated luminosities of 67 pb^{-1} (CDF: 19 pb^{-1} used in Ref. [4] and 48 pb^{-1} from the current Collider run which began early in 1994 and is expected to continue until the end of 1995) or 44−56 pb^{-1} (DØ: 13.5 pb^{-1} used in Ref. [7] and 30.5−42.5 pb^{-1}, depending on the channel, from the current Collider run), corresponding to $\sim 10^{13}$ inelastic $p\bar{p}$ collisions.

2 Tevatron Collider and Detectors

The Fermilab Tevatron Collider, with center-of-mass energy 1.8 TeV., is the highest energy collider in the world. It operates with 6 proton and 6 antiproton bunches, separated by electrostatic separators except at the B0 (CDF) and DØ interaction regions, where bunches cross every

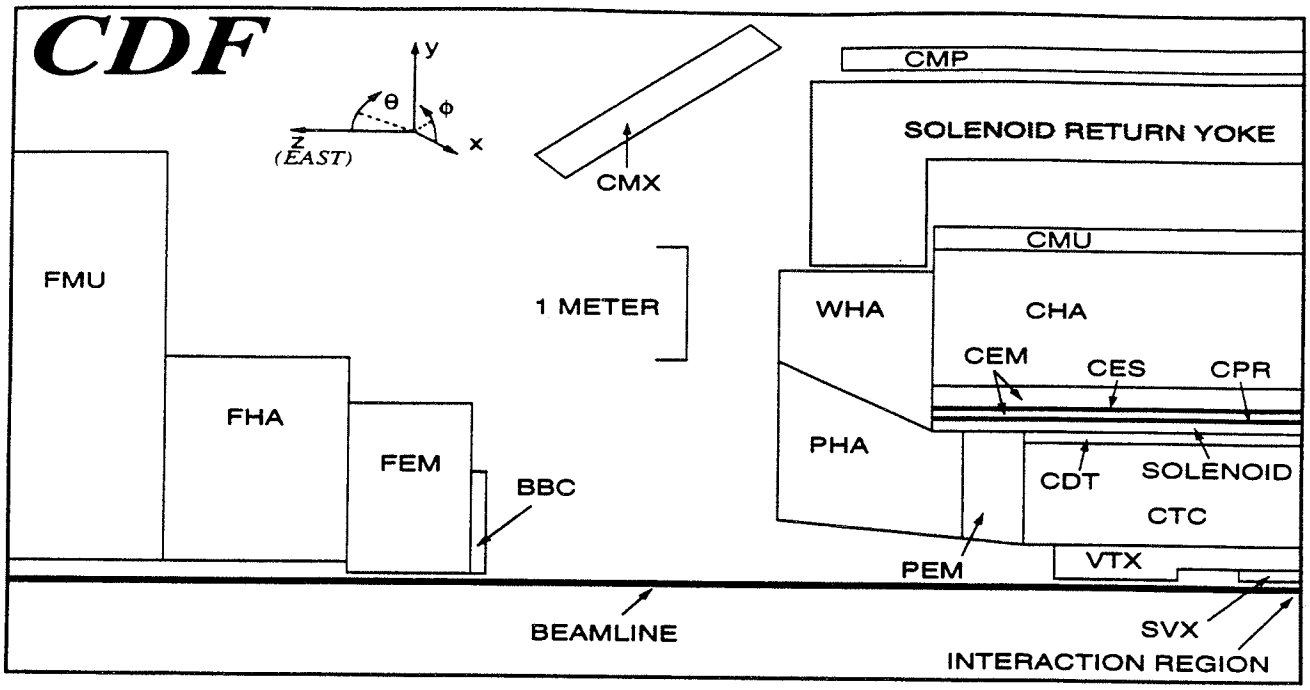

Figure 2: A side-view cross section of the CDF detector. The detector is forward-backward symmetric about the interaction region, which is at the lower-left corner of the figure.

3.5 μsec. The collision regions are long in the direction of the beams, with root-mean-square (rms) size $\sigma(z) \sim 30$ cm, while they are small, $\sigma(x \text{ or } y) \sim 36\mu$ in the directions perpendicular to the beams.

The CDF detector has been described in detail elsewhere[9]. The CDF detector consists of a magnetic spectrometer surrounded by calorimeters and muon chambers. A new low-noise, radiation-hard, four-layer silicon vertex detector, located immediately outside the beampipe, provides precise track reconstruction in the plane transverse to the beam and is used to identify secondary vertices from b and c quark decays[10]. The momenta of charged particles are measured in the central tracking chamber (CTC), which is in a 1.4-T superconducting solenoidal magnet. Outside the CTC, electromagnetic and hadronic calorimeters cover the pseudorapidity [3] region $|\eta| < 4.2$ and are used to identify jets and electron candidates. The calorimeters are also used to measure the missing transverse energy, $\not\!\!E_T$, which can indicate the presence of undetected energetic neutrinos. Outside the calorimeters, drift chambers in the region $|\eta| < 1.0$ provide muon identification. A schematic side view of the CDF detector is shown in Fig. 2. A three-level trigger selects the inclusive electron and muon events used in this analysis. To improve the $t\bar{t}$ detection efficiency, triggers based on $\not\!\!E_T$ are added to the lepton triggers used in Ref. [4].

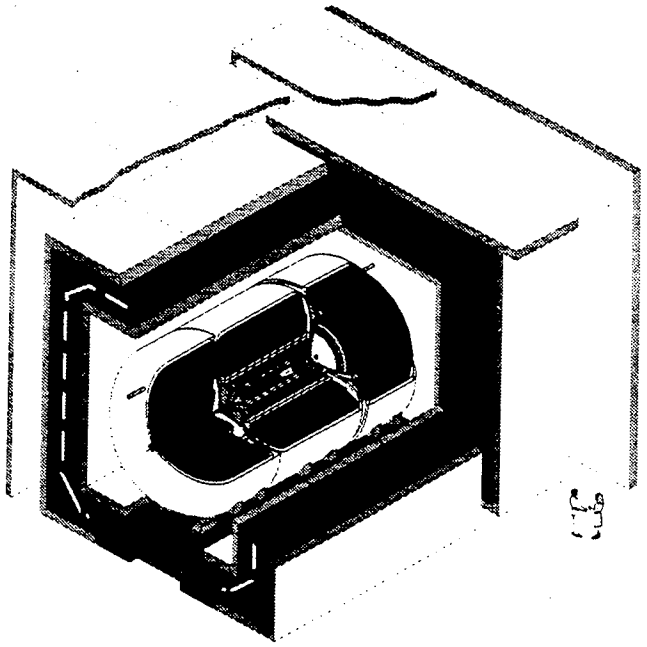

Figure 3: A schematic view of the DØ detector. The detector is forward-backward symmetric about the interaction region with good hermeticity and a large muon detector system.

The DØ detector and data collection systems are described in Ref. [11]. The DØ detector has a hermetic, compensating sampling calorimeter with fine longitudinal and transverse segmentation in pseudorapidity (η) and azimuth (ϕ). There is no central magnetic field. Charged particle tracks are reconstructed with a sign degeneracy using drift chambers located between the interaction region and calorimeter. Electrons are identified by a transition radiation detector. Muons are detected by reconstructing tracks in proportional drift tubes before and behind magnetized iron toroids located outside of the calorimeter. The bending angle of the track in the toroid determines the muon momentum, which is used to identify a low-momentum muon from a b semileptonic decay. A schematic view of the DØ detector is shown in Fig. 3.

3 Dilepton Search

The signature for the dilepton channel is characterized by two isolated leptons with opposite charges and high transverse momenta, large missing transverse energy $\not\!\!E_T$ due to two neutrinos, and two b-jets. The major backgrounds are Drell-Yan lepton pairs, $Z \rightarrow \tau\tau$, hadrons misidentified as leptons, WW, and $b\bar{b}$ production.

Cut	$e\mu$	ee	$\mu\mu$
P_T	39	2146	2220
Opposite-Charge	29	2118	2211
Isolation	25	2079	2148
Invariant Mass	25	215	233
$\not\!\!E_T$ magnitude	9	6	11
$\not\!\!E_T$ direction	9	5	4
Two-jet	5	0	2

Table 1: Number of data events surviving consecutive requirements (CDF)

3.1 CDF Dilepton Search

The CDF dilepton sample consists of inclusive lepton events containing an isolated electron with $E_T > 20$ GeV or an isolated muon with $P_T > 20$ GeV/c in the central region ($|\eta| < 1.0$), that also have a second lepton with $P_T > 20$ GeV/c, satisfying looser lepton identification requirements. The two leptons must have opposite electric charge. Events are removed as possible Z bosons if an ee or $\mu\mu$ invariant mass is between 75 and 105 GeV/c^2. The dilepton data sample is reduced by additional requirements on $\not\!\!E_T$ and the number of jets. In order to suppress background from Drell-Yan lepton pairs, which have little or no true $\not\!\!E_T$, the $\not\!\!E_T$ is corrected to account for jet energy mismeasurement [4]. The magnitude of the corrected $\not\!\!E_T$ is required to be at least 25 GeV. For the events with $\not\!\!E_T < 50$ GeV, the azimuthal angle between the $\not\!\!E_T$ vector and the nearest lepton or jet must be greater than 20° to reduce backgrounds from $Z \rightarrow \tau\tau$ with a subsequent $\tau \rightarrow l\nu\nu$ decay and Drell-Yan events with $\not\!\!E_T$ induced by jet mismeasurement. Finally, all events are required to have at least two jets with observed $E_T > 10$ GeV and $|\eta| < 2.0$.

As shown in Fig. 4 CDF observes a total of 7 dilepton events (5 for $e\mu$, 0 for ee, and 2 for $\mu\mu$) after all the cuts. Table 1 shows the number of dilepton events surviving consecutive requirements. The relative numbers are consistent with the dilepton acceptance, 60% of which is in the $e\mu$ channel. Although the expected background from radiative Z decay is estimated to be small (0.04 event), one of the $\mu\mu$ events contains an energetic photon with a $\mu\mu\gamma$ invariant mass of 86 GeV/c^2. To be conservative, CDF have removed that event from the final sample, which thus contains 6 events. Three of these events contain a total of 5 b-tags, compared with an expected 0.5 if the events are background. 3.6 tags would be expected if the events are

from $t\bar{t}$ decay. The total background expected is 1.3±0.3 events; 0.44±0.28 Drell-Yan lepton pairs, 0.38±0.07 $Z \rightarrow \tau\tau$, 0.23±0.15 hadrons misidentified as leptons, 0.21±0.07 WW, and 0.03±0.02 $b\bar{b}$ production. The first backgrounds are calculated from data and the last two with Monte Carlo simulation [4]. The probability of the background fluctuating to ≥ 6 events is calculated to be 3×10^{-3}, which corresponds to 2.7 standard deviations for a Gaussian probability distribution. Table 3 summarizes the CDF dilepton results.

3.2 DØ Dilepton Search

The DØ dilepton sample is made by similar requirements. The kinematic requirements are summarized in Table 2. For ee+jets events, $\not\!\!E_T > 40$ GeV is required to remove backgrounds from $Z \rightarrow ee$ if $|M_{ee} - M_Z| < 12$ GeV/c^2, where M_{ee} is the dielectron invariant mass. Events in $\mu\mu$+jets are required to be inconsistent with Z+jets hypothesis, based on a global kinematic fit. To improve background rejection, a minimum requirement on a quantity H_T, a scalar sum of the transverse energies E_T of the jets (for the single-lepton and $\mu\mu$+jets channels) or the scalar sum of the E_T's of the leading electron and the jets (for the $e\mu$+jets and ee+jets channels), is imposed. The H_T variable is a powerful discriminator between background and high-mass top quark production [8] (see Fig. 5). They have tested their understanding of background H_T distributions by comparing data and calculated background in background-dominated channels such as electron+two jets and electron+three jets. The observed H_T distribution agrees with the background calculation, which includes contributions from W+jets as calculated by the VECBOS Monte Carlo [12] and multijet events.

Kinematic Requirement	$e\mu$ + jets	ee + jets	$\mu\mu$ + jets
Lepton $E_T(e)$ or $P_T(\mu)$	15(e)/12(μ)	20/20	15/15
Missing E_T ($\not\!\!E_T$)	20	25	–
Number of Jets	2	2	2
Jet E_T	15	15	15
H_T	120	120	100

Table 2: Minimum kinematic requirements for the DØ dilepton event selection (energy in GeV)

As shown in Fig. 6 DØ observes a total of 3 dilepton events, 2 $e\mu$ and 1 $\mu\mu$, after all the cuts. No ee event is observed after the minimum H_T requirement of 120 GeV. The total background expected is 0.65±0.15 events. The significance of the excess corresponds to 1.9 standard deviations for a Gaussian probability distribution. Table 3 summarizes the DØ

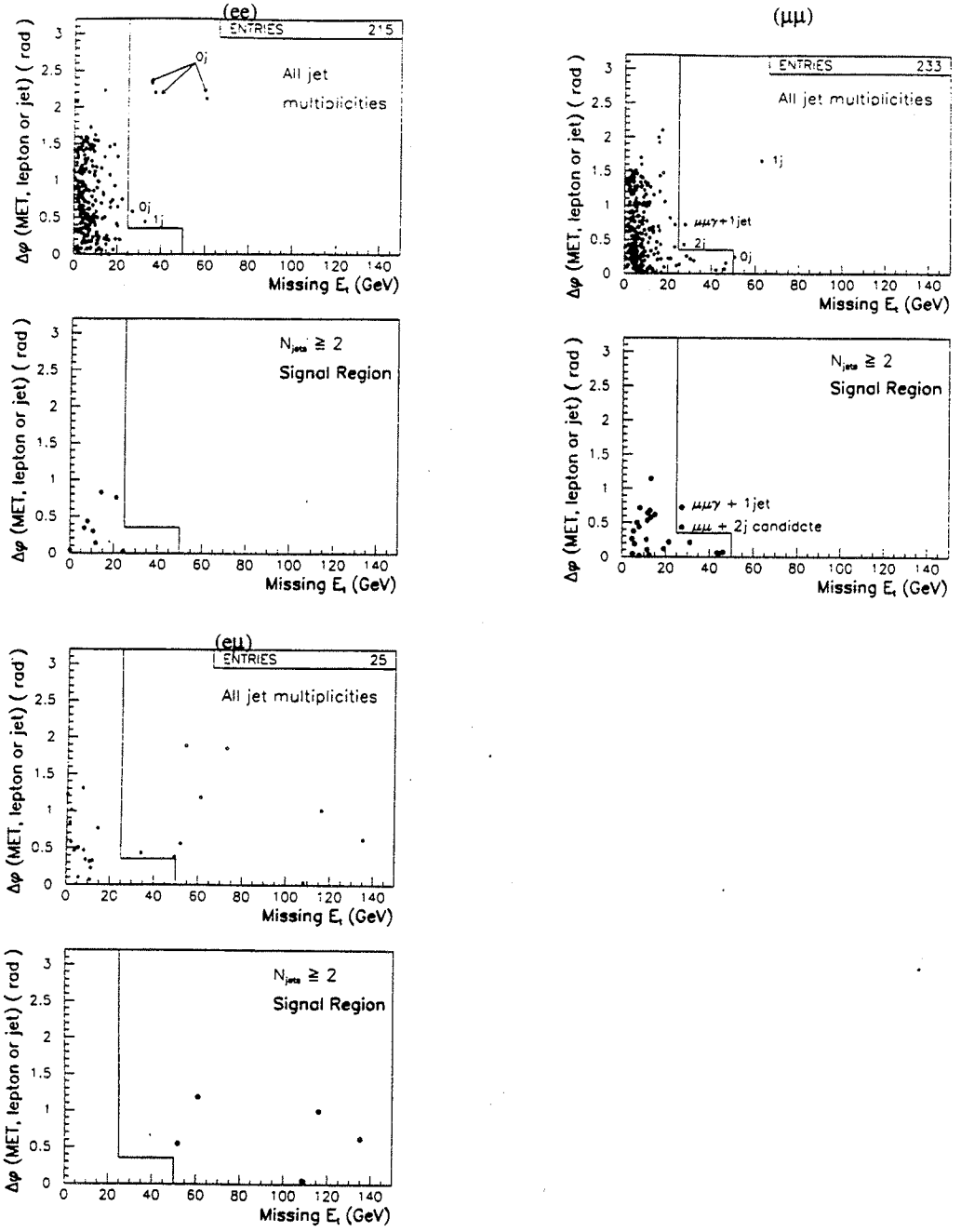

Figure 4: Distributions of the azimuthal angle between $\not\!\!E_T$ and the closest lepton or jet versus $\not\!\!E_T$ from CDF ee, $\mu\mu$, and $e\mu$ data before and after the two jet cut.

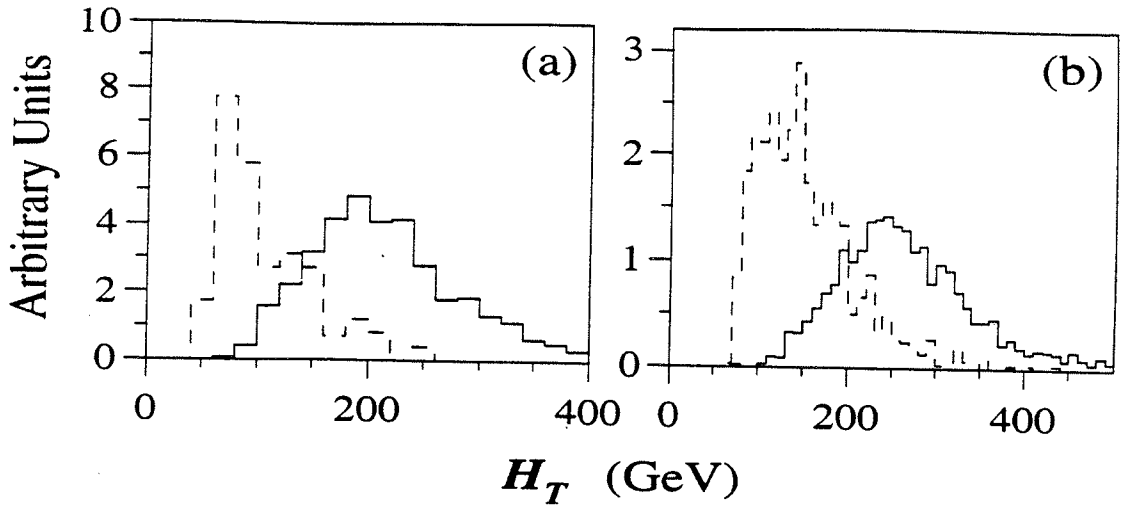

Figure 5: Shape of H_T distributions expected for the principal backgrounds (dashed histogram) and 200 GeV/c^2 top quarks (solid histogram) for (a) $e\mu$+jets and (b) untagged single-lepton+jets.

Experiment		$e\mu$	ee	$\mu\mu$	Total
CDF	$\int \mathcal{L}dt$ (pb^{-1})	67±8	67±8	67±8	
	Data	5	0	1	6
	Background	0.45±0.14	0.41±0.19	0.43±0.20	1.3±0.3
DØ	$\int \mathcal{L}dt$ (pb^{-1})	47.9±5.7	55.7±6.7	44.2±5.3	
	Data	2	0	1	3
	Background	0.12±0.03	0.28±0.14	0.25±0.20	0.65±0.15

Table 3: Summary of the dilepton results with the expected backgrounds

dilepton results.

4 Lepton+Jets Search

The $t\bar{t}$ decay signal in the lepton+jets channel is expected to have a single e or μ, missing transverse energy $\not\!\!E_T$ from a neutrino, two jets from a W decay, and two b-jets.

4.1 CDF Lepton+Jets Search

The CDF lepton+jets event sample is obtained by selecting $W \to e\nu$ and $W \to \mu\nu$ events in which an isolated electron (muon) is required to have $E_T \geq 20$ GeV ($P_T \geq 20$ GeV/c)

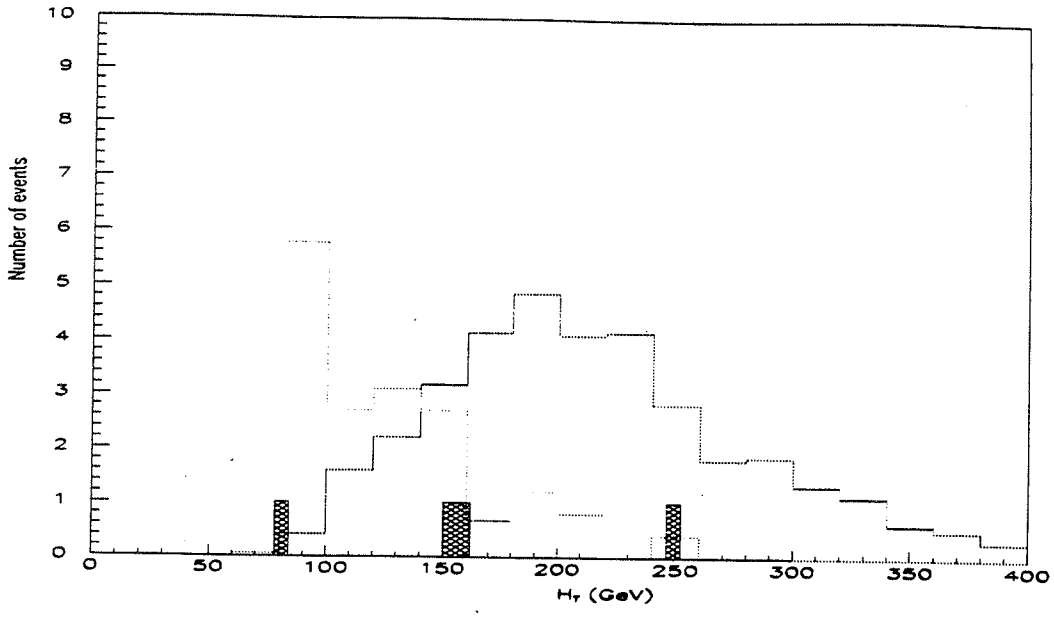

Figure 6: H_T distribution of the DØ dilepton candidate events (shaded histograms). 2 $e\mu$ events with $H_T > 120$ GeV, 1 $\mu\mu$ event with $H_T > 100$ GeV, and 1 ee event failing the minimum H_T requirement of 120 GeV. Shape of H_T distributions (dotted histograms) expected for the principal backgrounds (lower mean) and 200 GeV/c^2 top quarks (higher mean) for $e\mu$ events.

and to pass lepton identification cuts. An inclusive W boson sample is made by requiring $\not\!\!E_T > 20$ GeV after Z event removal. Table 4 classifies the W events by the number of jets with observed $E_T > 15$ GeV and $|\eta| < 2.0$. The number of observed W+multijet events decreases by an approximate factor of α_s for each additional jet. In contrast, the $t\bar{t}$ decay to $WWb\bar{b} \rightarrow$ lepton + ν+ jets ($q\bar{q}b\bar{b}$) produces, on average, three or four reconstructed jets. The "signal region" with $W+ \geq 3$ jets retains most of the expected $t\bar{t}$ events (70% of the 175 GeV/c^2 top signal), while removing the large majority of W+multijet background events. CDF select 203 events with $W+ \geq 3$ jets in which about 30 $t\bar{t}$ events are expected in the 67 pb^{-1} data for a top quark mass of 175 GeV/c^2. Therefore, additional background rejection is needed.

To obtain a further reduction of the QCD W+multijet background, CDF looks for b quarks in W+jet events by two different methods. The first method makes use of the new Silicon Vertex Detector (SVX)[10] to find secondary displaced-vertices from b quark decay (SVX tagging) based on b-hadron lifetime of $c\tau \sim 450\mu$. The vertex-finding efficiency is significantly larger now than previously due to an improved vertex-finding algorithm and the performance of the new vertex detector. The previous vertex-finding algorithm searched for a secondary vertex with 2 or more tracks. The new algorithm first searches for vertices with 3 or more tracks with looser track requirements, and if that fails, searches for 2-track vertices using more stringent

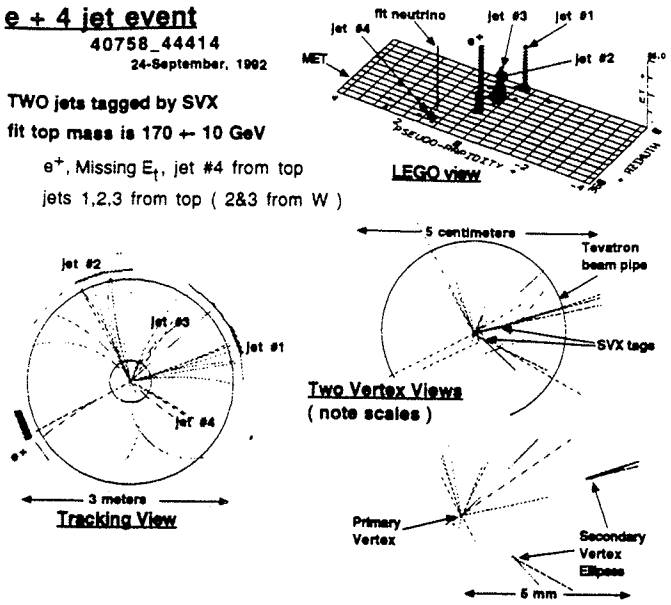

Figure 7: Event display for one of the e+4 jet events with two b-jets tagged by SVX; (a) observed calorimeter E_T is displayed in the $\eta - \phi$ plane, (b) the reconstructed tracks are shown in the central tracking chamber, and (c) the reconstructed SVX tracks are shown in the enlarged scale. Two of jets are found to have displaced vertices, which are consistent with coming from b-decay.

track and vertex quality criteria. The efficiency for tagging a b quark is measured in inclusive electron muon samples which are enriched in b decays. The ratio of the measured efficiency to the prediction of a detailed Monte Carlo is 0.96 ± 0.07, with good agreement ($\pm 2\%$) between the electron and muon samples. The efficiency for tagging at least one b quark in a $t\bar{t}$ event with ≥ 3 jets is determined from Monte Carlo to be $(42 \pm 5)\%$ in the current run, compared to the $(22 \pm 6)\%$ reported in the previous publication[13]. The results presented here are based on applying the new vertex finding algorithm to the data from the previous and the current runs. Fig. 7 shows an electron+4 jet event with two jets identified as b-jets by SVX tagging. The calorimeter and tracking detector views show an isolated electron, 4 jets and $\not\!\!E_T$. Two of the jets are found to have displaced vertices, 2.2 mm and 4.5 mm from the primary vertex, which are consistent with coming from b-decay (see a further magnified view of the event in Fig. 8). The remaining two jets make an invariant mass 79 GeV/c^2 consistent with the W boson mass. Therefore, this event is most likely from $t\bar{t} \rightarrow W^+ b W^- \bar{b} \rightarrow e^+ \nu b q \bar{q} \bar{q}$.

In Ref. [4], two methods were presented for estimating the background to the top quark signal. In method 1, the observed tag rate in inclusive jet samples is used to calculate the background from mistags and QCD-produced heavy quark pairs ($b\bar{b}$ and $c\bar{c}$) recoiling against a W boson. This is an overestimate of the background because there are sources of heavy quarks in an inclusive jet sample that are not present in W+jet events. In method 2, the mistag rate

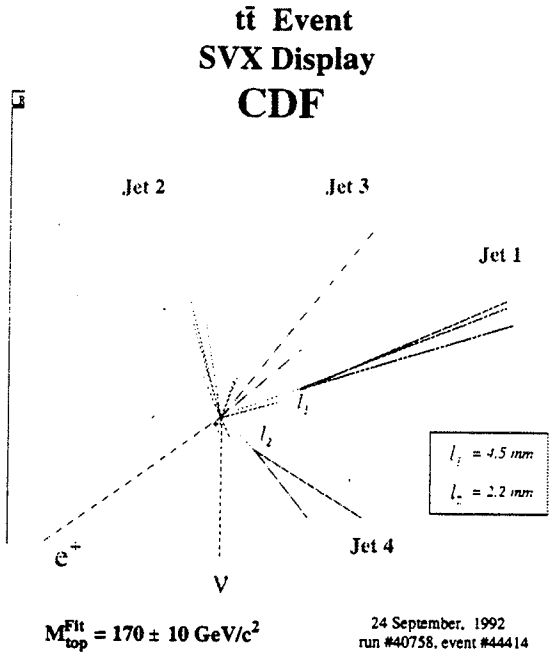

Figure 8: Silicon vertex detector (SVX) view of an e^+ + missing transverse energy ($\not\!\!E_T$) + 4 jets event observed by CDF. Two jets are identified as b-quarks by the SVX, and the rest two jets make an invariant mass 79 GeV/c^2 consistent with the W boson mass. Therefore, this event is most likely from $t\bar{t} \to W^+bW^-\bar{b} \to e^+\nu bq\bar{q}\bar{q}$.

is again measured with inclusive jets, while the fraction of W+jet events that are $Wb\bar{b}$ and $Wc\bar{c}$ is estimated from a Monte Carlo sample, using measured tagging efficiency. In the present analysis, CDF use method 2 as the best estimate of the SVX-tag background. The improved performance of the new vertex detector, our ability to simulate its behavior accurately, and the agreement between the prediction and data in the W+1 jet and W+2 jet samples make this a natural choice. The calculated background, including the small contributions from non-W background, Wc production, and vector boson pair production, is given in Table 4.

The numbers of SVX tags in the 1-jet and 2-jet samples are consistent with the expected

N_{jet}	observed events	observed SVX tags	background tags expected
1	6578	40	50±12
2	1026	34	21.2±6.5
3	164	17	5.2±1.7
≥4	39	10	1.5±0.4

Table 4: Number of lepton+jet events in the 67 pb^{-1} CDF data sample along with SVX tags observed and estimated background. Based on the excess number of tags in events with ≥ 3 jets, it is expected to have an additional 0.5 and 5 tags from $t\bar{t}$ decay in the 1 and 2 jets bins respectively.

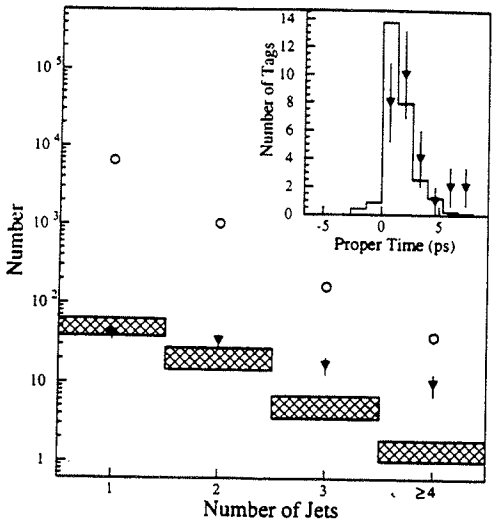

Figure 9: Number of events before SVX tagging (circles), number of tags observed (triangles), and expected number of background tags (hatched) versus jet multiplicity. Based on the excess number of tags in events with ≥ 3 jets, it is expected to have an additional 0.5 and 5 tags from $t\bar{t}$ decay in the 1 and 2 jet bins respectively. The inset shows the secondary vertex proper time distribution for 27 tagged jets in the $W+ \geq 3$-jet data (triangles) compared to the expectation for b quark jets from $t\bar{t}$ decay.

background plus a small $t\bar{t}$ contribution (Table 4 and Figure 9). However for the $W+ \geq 3$-jet signal region, 27 tags are observed compared to a predicted background of 6.7 ± 2.1 tags. The probability of the background fluctuating to ≥ 27 is calculated to be 2×10^{-5}, corresponding to 4.0 standard deviations for a Gaussian probability distribution, using the procedure outlined in Ref. [4]. The 27 tagged jets are in 21 events; the 6 events with 2 tagged jets can be compared with 4 expected for the top+background hypothesis and ≤ 1 for background alone. Fig. 9 also shows the decay lifetime distribution for the SVX tags in $W+ \geq 3$-jet events. It is consistent with the distribution predicted for b decay from the $t\bar{t}$ Monte Carlo simulation.

The second method for tagging b quarks (SLT tagging) is to look for an additional non-isolated lepton arising from the semileptonic b decay. Electrons and muons are found by matching CTC tracks with electromagnetic energy clusters or track segments in the muon chambers. To maintain acceptance for leptons coming directly from b decay and from the daughter c quark, the P_T threshold is kept low (2 GeV/c). The only significant change to the selection algorithm compared to the selection algorithm compared to Ref. [4] is that the fiducial region for SLT muons has been increased from $|\eta| < 0.6$ to $|\eta| < 1.0$, resulting in an increase of the SLT total acceptance and background by a factor of 1.2.

The major backgrounds in the SLT analysis are hadrons that are misidentified as leptons, and electrons from unidentified photon conversions. These rates and the smaller $Wb\bar{b}$ and $Wc\bar{c}$

Selection Cut	e+jets	μ+jets	e+jets/μ b-tag	μ+jets/μ b-tag
Lepton P_T	> 20 GeV	> 15 GeV	> 20 GeV	> 15 GeV
$\not\!\!E_T$	> 25 GeV	> 20 GeV	> 20 GeV	> 20 GeV
Number of Jets	≥ 4	≥ 4	≥ 3	≥ 3
Jet E_T	> 15 GeV	> 15 GeV	> 20 GeV	> 20 GeV
Aplanarity $\mathcal{A}$	> 0.05	> 0.05	> 0.00	> 0.00
H_T	> 200 GeV	> 200 GeV	> 140 GeV	> 140 GeV
μ-tag P_T	–	–	> 4 GeV	> 4 GeV

Table 5: Minimum kinematic requirements for the DØ standard lepton+jets event selection.

backgrounds are determined directly from inclusive jet data. The remaining backgrounds are much smaller and are calculated using the techniques discussed in Ref. [4]. The efficiency of the algorithm is measured with photon conversion and $J/\psi \rightarrow \mu^+\mu^-$ data. The probability of finding an additional e or μ in a $t\bar{t}$ event with ≥ 3 jets is (20±2)%. Table 6 shows the background and number of observed tags for the signal region ($W+ \geq 3$ jets). There are 23 tags in 22 events, with 15.4±2.0 tags expected from background. Six events contain both an SVX and SLT tag, compared to the expected 4 for top+background and 1 for background alone.

4.2 DØ Lepton+Jets Search

The DØ lepton+jets analysis consists of two methods: tight kinematic cuts for the events without b-tag, and loose kinematic cuts for the events with b-tag. The DØ b-tag technique is to search for a muon from semileptonic b decay with the minimum transverse momentum of 4 GeV/c. The lepton+jets sample is obtained by selecting events with one isolated lepton (e or μ), large $\not\!\!E_T$, and a minimum of three jets with $E_T > 20$ GeV (with muon b-tag) or four jets with $E_T > 15$ GeV (without muon b-tag). To reduce further the QCD-W+multijet background, a minimum requirement on the H_T quantity is imposed. A minimum requirement on the "aplanarity" of the jets $\mathcal{A}$, which measures the deviation from a planar momentum distribution and is proportional to the lowest eigenvalue of the momentum tensor for the observed objects (0.5: spherical events, 0.0: planar or linear events), is imposed for the lepton+jets without muon b-tag. Table 5 summarizes kinematic requirements for the lepton + jets event selection.

As shown in Fig. 10 DØ observes a total of 8 events (5 e+jets and 3 μ+jets) without μ b-tag after the tight kinematic kinematic cuts. The total expected background is 1.93±0.55. The

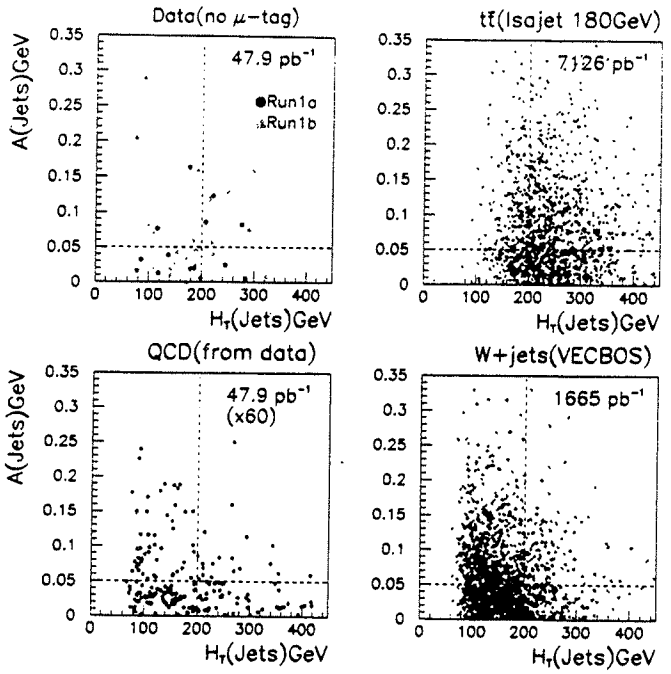

Figure 10: Aplanarity ($\mathcal{A}$) vs. H_T distributions for (a) DØ data (top left), (b) 180 GeV/c^2 top Monte Carlo (ISAJET) (top right), (c) background predicted from QCD data (bottom left), and (d) background predicted from W+jets Monte Carlo (VECBOS) (bottom right).

backgrounds in the signal region from W+jets, hadrons misidentified as leptons, and Z+jets are estimated from the single-lepton+1 or 2 jet data based on a scaling constant for an additional jet.

The number of observed single-lepton+jets events with a μ b-tag is shown as a function of minimum jet multiplicity in Fig. 12. For the $W+ \geq$ 3-jet signal region, 6 events are observed compared to a predicted background of 1.2±0.2. Fig. 11 shows an electron+4 jet event with two soft muons found in a jet. The two soft (both with 6±1 GeV/c) muons make an invariant mass of 720 MeV/c^2 consistent with coming from a sequential decay $b \to c\mu^-\nu \to s\mu^+\nu\mu^-\nu$.

5 Summary of Counting Experiments

In summary, CDF finds 37 b-tagged $W+ \geq$ 3-jet events (21 events with SVX tags and 22 events with SLT tags; 6 of these events with both SVX and SLT tags) that contain 27 SVX tags compared to 6.7±2.1 expected from background and 23 SLT tags with an estimated

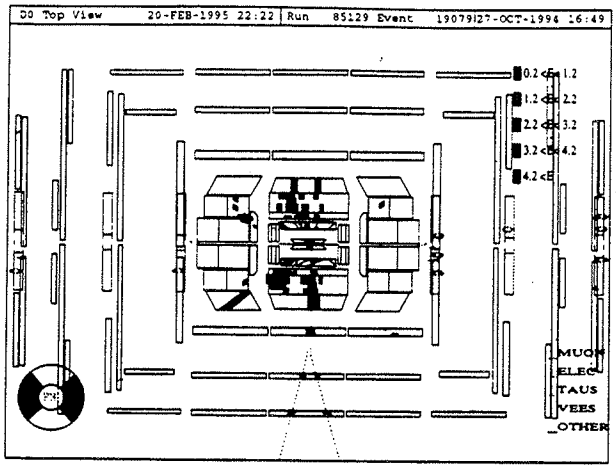

Figure 11: Event display for one of the DØ E+4 jet events with a μ b-jet. Two soft muons with opposite charges are found in a jet, which is consistent with coming from a sequential decay $b \to c\mu^-\nu \to s\mu^+\nu\mu^-\nu$.

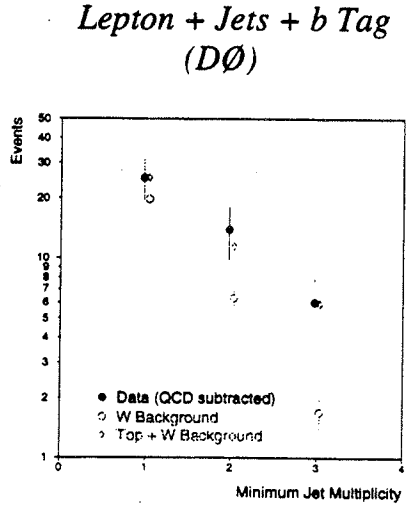

Figure 12: Minimum jet multiplicity distributions for single-lepton+jets events with μ b-tag (solid circles), the predicted W+multijet background (open circles), and the background plus expected 200 GeV/c^2 top signal (open diamonds).

	Channel	SVX	SLT	Dilepton	Total
	Data	27 tags	23 tags	6 events	43 events
CDF	Background	6.7±2.1	15.4±2.0	1.3±0.3	
	Probability	2×10^{-5} (4.6σ)	6×10^{-2} (1.9σ)	3×10^{-3} (2.7σ)	1×10^{-6} (4.8σ)
	Channel	l+jets	l+jets with b-tag	Dilepton	Total
	Data	8 events	6 events	3 events	17 events
DØ	Background	1.9±0.5	1.2±0.2	0.7±0.2	3.8±0.6
	Probability	2×10^{-3} (2.9σ)	2×10^{-3} (2.9σ)	3×10^{-2} (1.9σ)	2×10^{-6} (4.6σ)

Table 6: Summary of the results of counting experiments with the observed events, the expected backgrounds and the significances of the excesses.

background of 15.4±2.0. There are 6 dilepton events compared to 1.3±0.3 events expected from background. The combined probability of a background fluctuation to the number of observed events or more is calculated to be 1×10^{-6}, which is equivalent to a 4.8σ deviation in a Gaussian distribution. From the number of SVX tagged events, the estimated background, the calculated $t\bar{t}$ acceptance, and the integral luminosity of the data sample, CDF calculates the $t\bar{t}$ production cross section to be $6.8^{+3.6}_{-2.4}$ pb, where the uncertainty includes both statistical and systematic effects.

From all seven channels, DØ observes 17 events with an expected background of 3.8±0.6 events (see Table 6). The measured cross section as a function of the top quark mass hypothesis is shown in Fig. 13. Assuming a top quark mass of 200 GeV/c^2, the production cross section is 6.3±2.2 pb. The error in the cross section includes an overall 12% uncertainty in the luminosity. The probability of an upward fluctuation of the background to 17 or more events is 2×10^{-6}, which corresponds to 4.6σ for a Gaussian probability distribution.

6 Top-Quark Mass Determination

Single lepton events with 4 or more jets can be kinematically reconstructed to the $t\bar{t} \rightarrow WbW\bar{b}$ hypothesis, yielding for each event an estimate of the top quark mass [4]. The lepton, neutrino ($\not\!\!E_T$), and the fourth highest-E_T jets are assumed to be the $t\bar{t}$ daughters through the following processes:

$$p\bar{p} \rightarrow t_1 + t_2 + X$$
$$t_1 \rightarrow W_1 + b_1$$

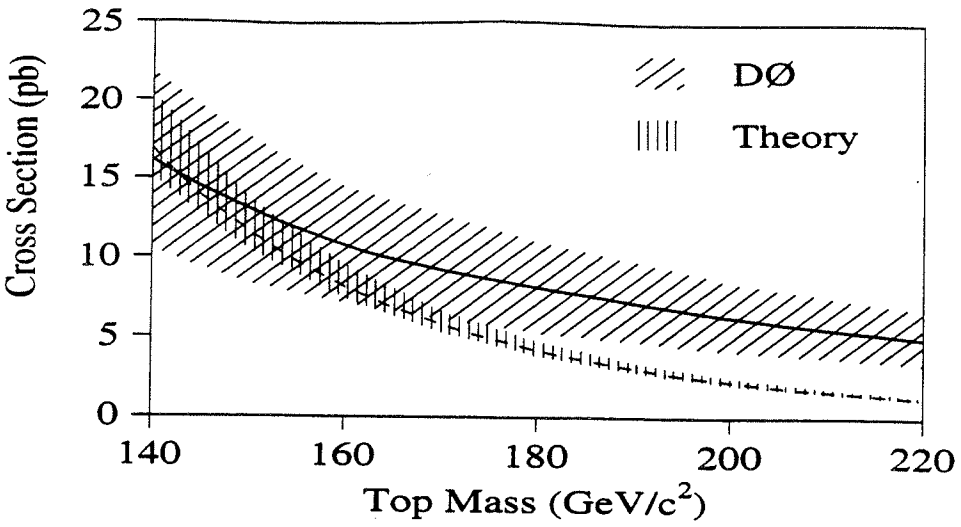

Figure 13: DØ measured $t\bar{t}$ production cross section (solid line with one standard deviation error band) as a function of assumed top quark mass. Also shown is the theoretical cross section curve (dashed line).

$$t_2 \rightarrow W_2 + b_2$$
$$W_1 \rightarrow l + \nu$$
$$W_2 \rightarrow j_1 + J_2$$

where X represents additional particles produced in the process and the lepton (l) is e or μ. This is a 2-constraint fit in that there are a total of 52 variables (the four-vectors of 13 particles), 34 measured (or known) quantities, and 20 equations of momentum conservation for 5 processes. One can reconstruct the t and $\bar{t}$ by fitting the entire event subject to the following constraints: (1) the momenta and energies of particles at every decay process must satisfy their conservation laws, (2) the lepton plus neutrino and the quark plus antiquark from W decays must reconstruct to the W mass ($M_{jj} = M_W$ and $M_{l\nu} = M_W$), (3) the t and $\bar{t}$ are required to have the equal mass ($M_t = M_{\bar{t}}$). Unfortunately one cannot tell *a priori* which two jets are from the hadronic W decay and which two jets are from b quarks. If the event contains additional jets, only the four highest-E_T jets are used in the fit. There is a quadratic sign ambiguity in determining the longitudinal momentum of the neutrino. As a result one must fit the event assuming all possible identities for each quark jet and both solutions for the neutrino momentum. There are 24 possible combinations. If one of the two b-quarks are identified correctly, there are 12 possible combinations.

6.1 CDF Mass Determination

For each event, the solution with the lowest fit χ^2 is chosen. Starting with the 203 events with ≥ 3 jets, CDF requires each event to have a fourth jet with $E_T > 8$ GeV and $|\eta| < 2.4$. This yields a sample of 99 events, of which 88 pass a loose χ^2 requirement ($\chi^2 < 10$) on the fit. When the fitting method is applied to $t\bar{t}$ events generated by the HERWIG program [14] at a top mass of 170 GeV/c^2, the reconstructed mass distribution peaks near the input mass, as shown in Fig. 14. For comparison, applying the method to background W+jets events generated by the VECBOS program [12], leads to the broad distribution, peaked near 140 GeV/c^2, shown in Fig. 14.

The reconstructed mass distribution for the 88 events is shown in Fig. 15. The distribution is consistent with the predicted mix of approximately 30% $t\bar{t}$ signal and 70% background. The Monte Carlo background shape agrees well with that measured in a limited-statistics sample of Z+4 jet events as well as in a QCD sample selected to approximate non-W background.

After requiring an SVX or SLT b-tag, 19 of the events remain, of which $6.9^{+2.5}_{-1.9}$ are expected to be background. For these events, only solutions in which the tagged jet is assigned to one of the b quarks are considered. Fig. 16 shows the mass distribution for the tagged events. The mass distribution in the current run is very similar to that from the previous run.

To find the most likely top mass, CDF fits the mass distribution to a sum of the expected distributions from the W+jets background and a top quark mass M_{top}. The -ln(likelihood) distribution from the fit is shown in the Fig. 16 inset. The best fit mass is 176 GeV/c^2 with a ± 8 GeV/c^2 statistical uncertainty. CDF make a conservative extrapolation of the systematic uncertainty from the previous publication, giving $M_{top} = 176 \pm 8 \pm 10$ GeV/c^2. Systematic uncertainties arise from the effects of gluon radiation on the determination of parton energies, the jet energy scale, kinematic bias in the tagging algorithm, and ambiguity in the mass templates. Further studies of systematic uncertainties are in progress.

6.2 DØ Mass Determination

Kinematic fits are performed on all permutations of the jet assignments of the four highest E_T jets, with the provision that muon-tagged jets are always assigned to a b-quark in the fit. A maximum of three permutations with $\chi^2 < 7$ are retained, and a single χ^2-probability-weighted average mass ("fitted mass") is calculated for each event. Monte Carlo studies using the ISAJET and HERWIG event generators showed that the fitted mass is strongly correlated with the top quark mass. Gluon radiation, jet assignment combinatorics, and the event selection procedure introduce a shift in the fitted mass (approximately -20 GeV/c^2 for 200 GeV/c^2 top quarks),

Mass Reconstruction for Top and W+jets Monte Carlo

Reconstructed mass for HERWIG MonteCarlo, $M_{top} = 170$ GeV

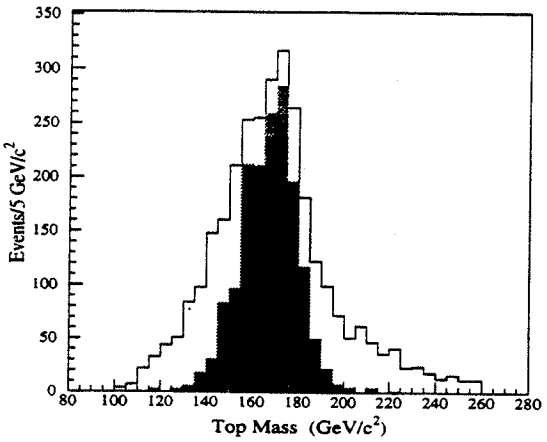

Reconstructed mass for the VECBOS+HERPRT W+3 jets events.

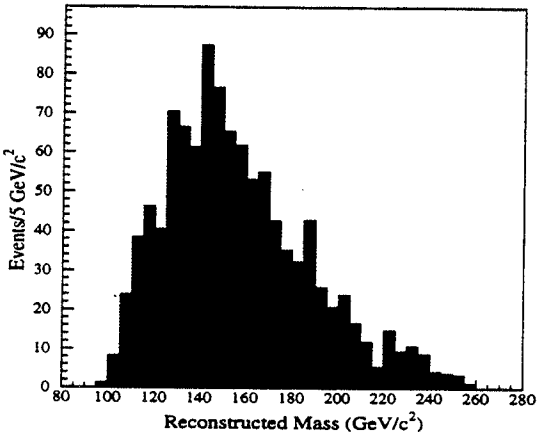

Figure 14: Reconstructed top masses for top and W+jets Monte Carlo samples. (a) Reconstructed top mass distribution for Monte Carlo events generated with top mass 170 GeV/c^2. The open histogram corresponds to the best fit obtained by the fitting program when requiring that one of the b-jets is a b in the fit. The shaded histogram refers to the fit with correct assignment for each of the jets. (b) Reconstructed mass distribution for W+multijet Monte Carlo (VECBOS) events.

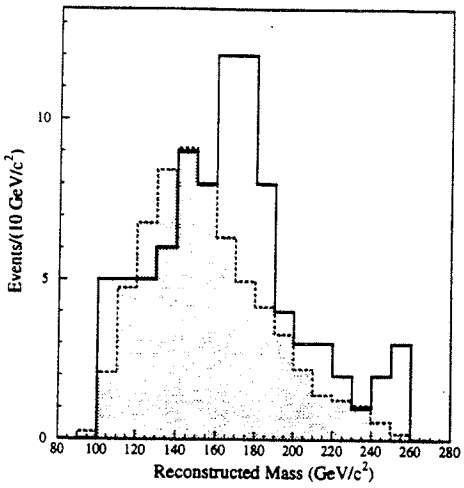

Figure 15: Reconstructed mass distribution for the $W+ \geq$ 4-jet sample prior to b-tagging (solid). Also shown is the background distribution (shaded), with the normalization constrained to the calculated value.

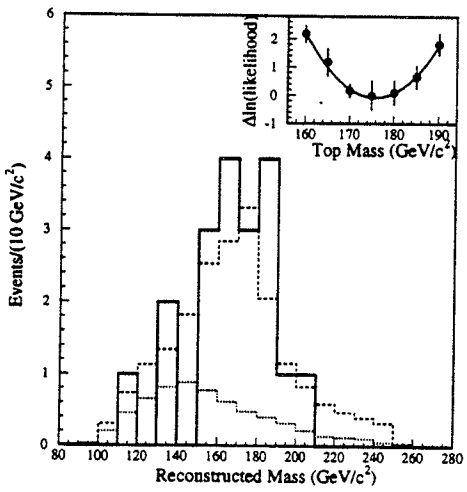

Figure 16: Reconstructed mass distribution for the b-tagged $W+ \geq$ 4-jet events (solid). Also shown are the background shape (dotted) and the sum of background plus $t\bar{t}$ Monte Carlo for top mass 175 GeV/c^2 (dashed), with the background constrained to the calculated value, $6.9^{+2.5}_{-1.9}$ events. The inset shows the likelihood fit used to determine the top mass.

which is taken into account in the final mass determination.

Eleven of the fourteen single-lepton+jets candidate events selected using the standard cuts are fitted successfully. Fig. 17 shows the fitted mass distribution. An unbinned likelihood fit, incorporating top quark and background contributions, with the top quark mass allowed to vary, is performed on the fitted mass distribution. The top quark contribution is modeled using ISAJET. The background contributions are constrained to be consistent with the background estimates. The likelihood fit yields a top quark mass of 199^{+31}_{-25}(stat.) GeV/c^2 and describes the data well.

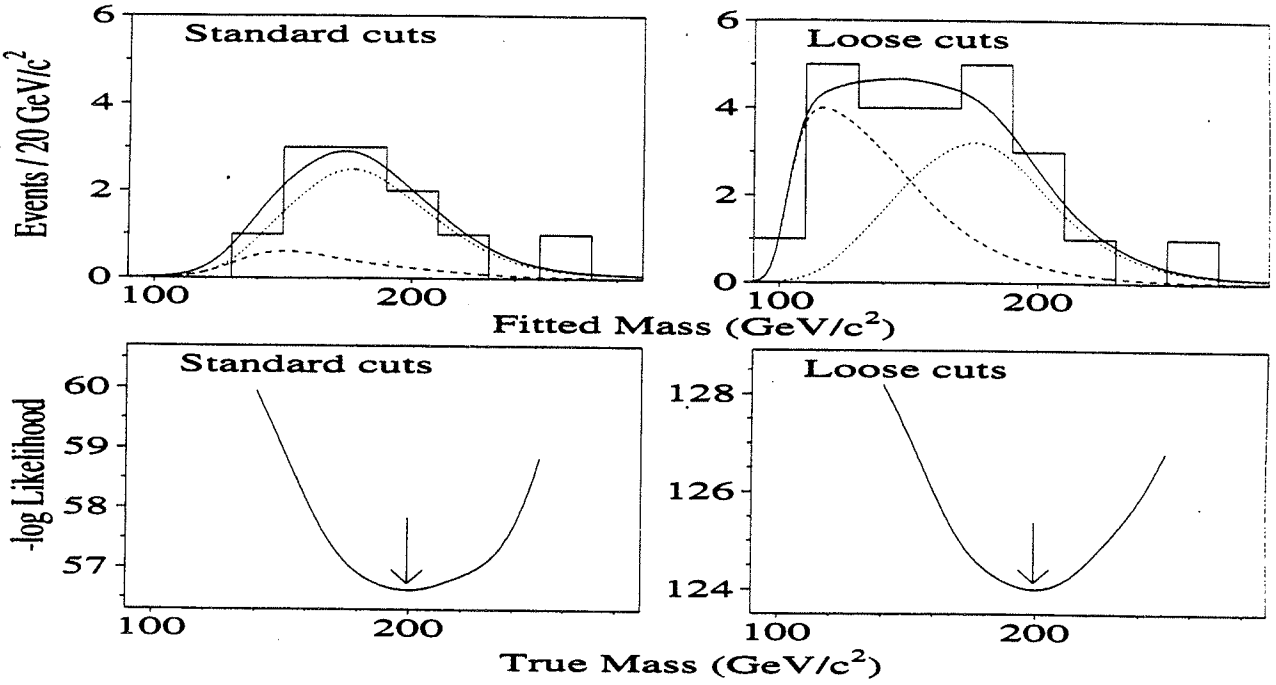

Figure 17: DØ fitted mass distribution for candidate events (histograms) with the expected mass distribution for 199 GeV/c^2 top quark events (dotted curve), background (dashed curve), and the sum of top and background (solid curve) for standard (11 events) and loose (24 events) event selections. A shift in the fitted mass (approximately -20 GeV/c^2 for 200 GeV/c^2 top quarks) distribution, which is introduced by gluon radiation, jet assignment combinatorics, and the event selection procedure, is taken into account in the final mass determination shown by the likelihood distributions.

To increase the statistics available for the mass fit, and to remove any bias from the standard H_T requirement, DØ repeats the mass analysis on the events selected using a set of loose event selection requirements, which differs from the standard set by the removal of the H_T requirement and by relaxation of the aplanarity requirement from $\mathcal{A} > 0.05$ to $\mathcal{A} > 0.03$. Of 27 single-lepton + 4-jet events, 24 are fitted successfully. The removal of the H_T requirement introduces a substantial background contribution at lower mass in addition to the top signal, as shown in Fig. 17. A likelihood fit to the mass distribution results in a top quark mass of 199^{+19}_{-21}(stat.) GeV/c^2, consistent with the result obtained from the standard event selection.

The result of the likelihood fit did not depend significantly on whether the normalization of the background is constrained. Using HERWIG to model the top quark contribution results in a mass 4 GeV/c^2 below that found using ISAJET. This effect is included in the systematic error. The total systematic error in the top quark mass is 22 GeV/c^2, which is dominated by the uncertainty in the jet energy scale.

7 Summary and Conclusions

Additional CDF data confirm the top quark evidence presented in Ref. [4]. There is now a large excess in the signal that is inconsistent with background prediction by 4.8σ, and a clear mass peak. In addition, a substantial fraction of the jets in the dilepton events are b-tagged. This establishes the existence of the top quark. The preliminary mass and cross section measurements yield $M_{top} = 176 \pm 8 \pm 10$ GeV/c^2 and $\sigma_{t\bar{t}} = 6.8^{+3.6}_{-2.4}$ pb.

D$\emptyset$ observes 17 events with an expected background of 3.8 ± 0.6 events. The probability of an upward fluctuation of the background to 17 or more events is 2×10^{-6}, which corresponds to 4.6σ for a Gaussian distribution. This also establishes the top quark. The mass and cross section measurements yield $M_{top} = 199^{+19}_{-21}$(stat.)$\pm$22(syst.) GeV/$c^2$ and $\sigma_{t\bar{t}} = 6.4 \pm 2.2$ pb at the measured top mass.

Therefore, the last building-block of SM, the top quark, is found by the CDF and D$\emptyset$ collaborations at Fermilab in 1995!

8 Prospects for Top-Quark Physics

All the building blocks of the standard model are now observed. However, the Higgs particle is not yet detected and the masses of neutrinos are not measured. The top quark may yield an answer to the question of what generates mass in the electroweak theory due to its heavy mass and strong coupling to the Higgs. According to the simplest standard model, which incorporates a single Higgs particle, the W boson and top-quark masses could be used to constrain the Higgs mass due to radiative corrections as shown in Fig. 18. In the future, improved measurements of W and top-quark masses would constrain the Higgs mass considerably.

The kinematic properties of top decays, such as the invariant $t\bar{t}$ mass, reconstructed from the top samples will provide opportunities to probe strong interaction dynamics at the top-mass scale and to search for exotic species, such as supersymmetric particles. Fig. 19 shows the reconstructed $t\bar{t}$ mass distribution of 19 b-tagged single-lepton+4 jet·top candidate events. While the distribution is consistent with that of the calculated background plus $t\bar{t}$ Monte Carlo

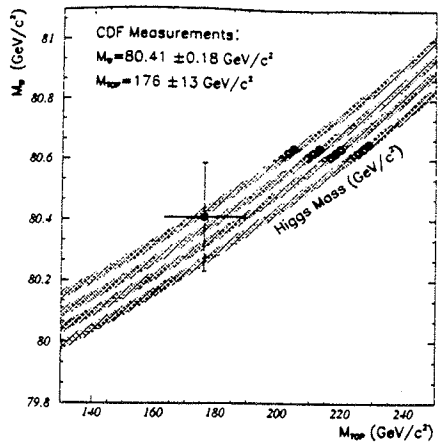

Figure 18: Possible Higgs masses as a function of the top and W masses shown by the band. The W mass is contributed by the electroweak radiative corrections due to the top and Higgs.

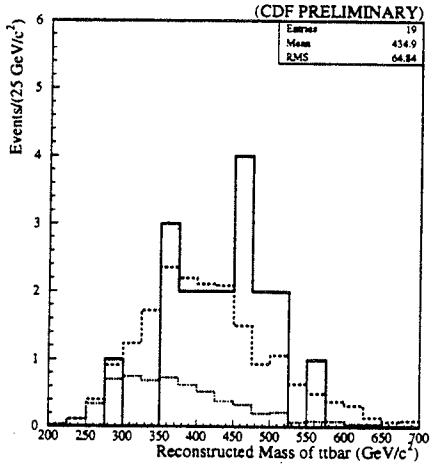

Figure 19: CDF reconstructed $t\bar{t}$ mass distribution of 19 b-tagged single-lepton+4 jet top candidate events (solid). Also shown are the background shape (dotted) and the sum of background plus $t\bar{t}$ Monte Carlo for top mass 175 GeV/c^2 (dashed).

for top mass 175 GeV/c^2, the number of candidate events is too few to exclude the possibility of resonance or an evidence for new phenomena.

According to the standard model, the W bosons from decays of 175-GeV/c^2 top quarks should be about 70% longitudinally polarized, and should be even more polarized for heavier top masses. Measuring the W polarization could serve as a probe of physics beyond standard model.

The numbers of reconstructed top events in the single and double b-tagged samples can be used to measure the CKM matrix element V_{tb}. Possible non-standard model physics can cause the branching fraction of $t \to Wb$ to deviate from unity.

Few would have imagined in 1977 when the b-quark was discovered that it would be interesting enough to produce copious B mesons at B factories. Therefore, the top-quark

physics is born in 1995, and its future will be every bit as unexpected and exciting as that being realized with the b quark.

References

[1] A. Bean *et al.*, Phys. Rev. **D35**, 3533 (1987).

[2] W. Bartel *et al.*, Phys. Lett. **146B**, 437 (1984).

[3] The pseudorapidity, η, is defined as $-\ln(\tan(\theta/2))$ where θ is the polar angle

[4] F. Abe *et al.*, Phys. Rev. **D50**, 2966 (1994); F. Abe *et al.*, Phys. Rev. Lett. **73**, 225 (1994).

[5] S. Abachi *et al.*, Phys. Rev. Lett. **72**, 2138 (1994).

[6] S. Abachi *et al.*, Phys. Rev. Lett. **74**, 2422 (1995).

[7] F. Abe *et al.*, Phys. Rev. Lett. **74**, 2626 (1995).

[8] S. Abachi *et al.*, Phys. Rev. Lett. **74**, 2632 (1995).

[9] F. Abe *et al.*, Nucl. Instrum. Methods Phys. Res., Sect. A **271**, 387 (1988).

[10] P. Azzi *et al.*, FERMILAB-CONF-94/205-E. The previous silicon vertex detector is described in D. Amidei *et al.*, Nucl. Instrum. Methods Phys. Res., Sect. A **350**, 73 (1994).

[11] S. Abachi *et al.*, Nucl. Instrum. Methods Phys. Res., Sect. A **338**, 185 (1994).

[12] W. Giele, E. Glover, and D. Kosower, Nucl. Phys. **B403**, 633 (1993).

[13] A factor of 1.65 increase comes from the improvement noted. The remaining factor of 1.15 results from correcting an error in the b baryon lifetime used in the simulation of $t\bar{t}$ decay in Ref. [4].

[14] G. Marchiesini and B.R. Webber, Nucl. Phys. **B310**, 461 (1988); G. Marchiesini *et al.*, Computer Phys. Comm. **67**, 465 (1992).